doi:10.1016/j.jmb.2010.08.015 J. Mol. Biol. (2010) 402, 638–644

Contents lists available at www.sciencedirect.com

Journal of Molecular Biology

journal homepage: http://ees.elsevier.com.jmb

COMMUNICATION

Magnesium-Dependent Interaction of PKR with Adenovirus VAI

Katherine Launer-Felty[1], C. Jason Wong[1], Ahmed M. Wahid[2], Graeme L. Conn[3] and James L. Cole[1,4]*

[1]*Department of Molecular and Cell Biology, University of Connecticut, Storrs, CT 06269, USA*
[2]*Department of Biochemistry, Faculty of Pharmacy, Minia University, Minia, Egypt*
[3]*Department of Biochemistry, Emory University School of Medicine, Atlanta, GA 30322, USA*
[4]*Department of Chemistry, University of Connecticut, Storrs, CT 06269, USA*

Received 25 June 2010; received in revised form 6 August 2010; accepted 9 August 2010
Available online 14 August 2010

Edited by D. E. Draper

Keywords:
analytical ultracentrifugation; innate immunity; protein–nucleic acid interactions; protein kinase

Protein kinase R (PKR) is an interferon-induced kinase that plays a pivotal role in the innate immunity pathway for defense against viral infection. PKR is activated to undergo autophosphorylation upon binding to RNAs that contain duplex regions. Activated PKR phosphorylates the α-subunit of eukaryotic initiation factor 2, thereby inhibiting protein synthesis in virus-infected cells. Viruses have evolved diverse PKR-inhibitory strategies to evade the antiviral response. Adenovirus encodes virus-associated RNA I (VAI), a highly structured RNA inhibitor that binds PKR but fails to activate. We have characterized the stoichiometry and affinity of PKR binding to define the mechanism of PKR inhibition by VAI. Sedimentation velocity and isothermal titration calorimetry measurements indicate that PKR interactions with VAI are modulated by Mg^{2+}. Two PKR monomers bind in the absence of Mg^{2+}, but a single monomer binds in the presence of divalent ion. Known RNA activators of PKR are capable of binding multiple PKR monomers to allow the kinase domains to come into close proximity and thus enhance dimerization. We propose that VAI acts as an inhibitor of PKR because it binds and sequesters a single PKR in the presence of divalent cation.

Viral infection activates the host innate immunity response, leading to the synthesis of type 1 interferons and subsequent induction of a large number of antiviral genes.[1] Among these, the double-stranded RNA (dsRNA)-activated protein kinase R (PKR) plays a dominant role.[2] The enzyme is induced in a latent form, but is activated by binding to dsRNA or RNAs containing duplex regions to undergo autophosphorylation. Activated PKR blocks cap-dependent translational initiation by phosphorylating the α-subunit of eukaryotic initiation factor 2 at serine 51. Thus, production of dsRNA during viral infection[3] results in PKR activation and inhibition of protein synthesis.

PKR contains an N-terminal dsRNA binding domain that consists of two tandem copies of the dsRNA binding motif[4] and a C-terminal kinase, with an ~90-aa interdomain linker lying between these domains. The structures of the isolated dsRNA binding domain[5] and a complex of the kinase domain with the α-subunit of eukaryotic initiation factor 2 have been solved.[6] The linker is flexible, and

**Corresponding author.* Department of Molecular and Cell Biology, University of Connecticut, 91 North Eagleville Road, U-3125, Storrs, CT 06269, USA.
E-mail address: james.cole@uconn.edu.

Abbreviations used: PKR, protein kinase R; VAI, virus-associated RNA I; dsRNA, double-stranded RNA; ITC, isothermal titration calorimetry.

0022-2836/$ - see front matter

PKR adopts multiple compact and extended conformations in solution.[7]

Dimerization plays a key role in PKR activation.[8,9] PKR dimerizes weakly in solution, and dimerization is sufficient to activate PKR in the absence of RNA.[10] Activation of PKR by dsRNA follows a "bell-shaped" curve where low RNA concentrations activate, but higher RNA concentrations inhibit.[11,12] These results can be rationalized in a model where low concentrations of dsRNA favor the assembly of multiple PKR monomers on a single dsRNA, whereas high dsRNA concentrations dilute PKR monomers onto separate molecules of dsRNA.[13] Consistent with the dimerization model, a minimum of 30 bp of dsRNA is required to bind two PKR monomers and to activate autophosphorylation, supporting a model where the role of dsRNA is to bring two or more PKR monomers in close proximity to enhance dimerization via the kinase domain.[14,15]

The importance of PKR in antiviral defense is underscored by the large number of viruses that produce PKR inhibitors and the variety of mechanisms used.[16] Adenovirus and Epstein–Barr virus encode RNA decoys that bind PKR but do not activate, thereby serving to block the antiviral response. Adenovirus virus-associated RNA I (VAI) is an ~160-nt RNA that accumulates to high concentration late in viral infection. VAI contains three major domains: the terminal stem, a complex central domain, and an apical stem loop (Fig. 1).[20,21] There is evidence that the central domain is stabilized by tertiary interactions and possibly forms a

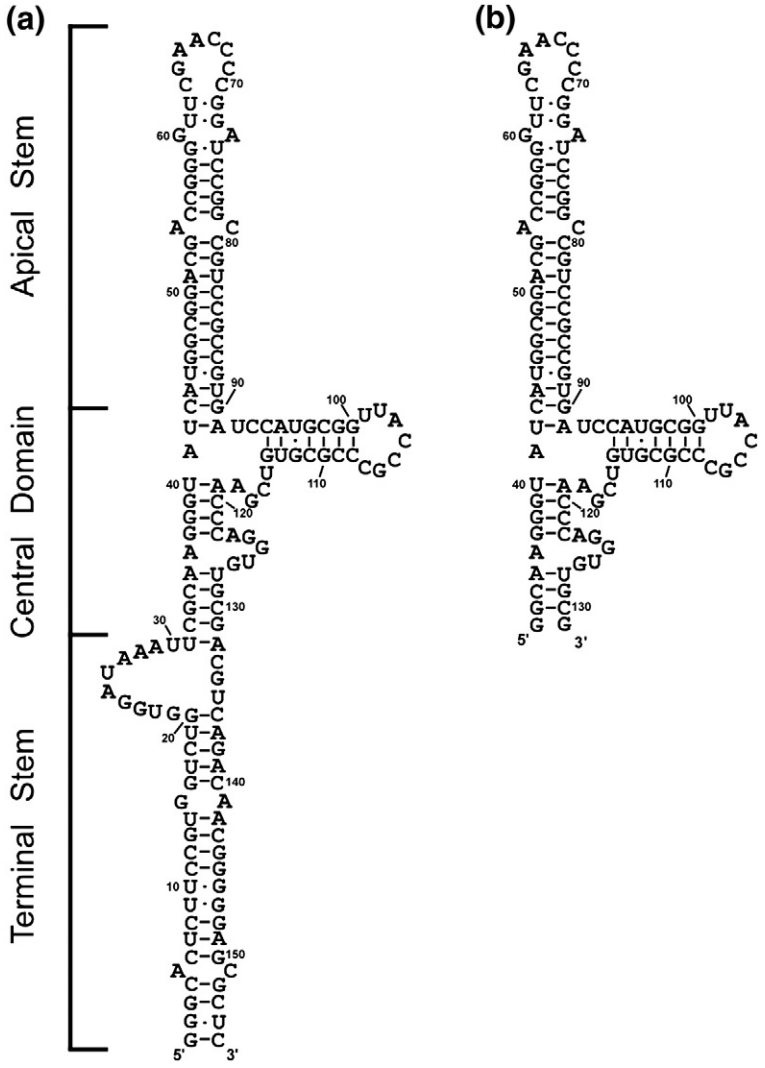

Fig. 1. Secondary structures of RNAs used in this study. (a) Wild-type VAI. (b) ΔTS mutant lacking the terminal stem. The secondary structures are based on enzymatic structure probing measurements.[17] RNAs were prepared by *in vitro* transcription from plasmid templates, as previously described,[18,19] and purified on preparative denaturing gels, then electroeluted. The RNAs were annealed by heating to 90 °C, then snap cooled.

pseudoknot.[22] Early enzymatic structure probing measurements[23] suggested that Mg^{2+} alters VAI conformation, but it was recently reported that melting of VAI is insensitive to divalent ion.[18,24] The binding sites for PKR have been mapped to the apical stem and the central domain.[17,20,21,23,25–29]

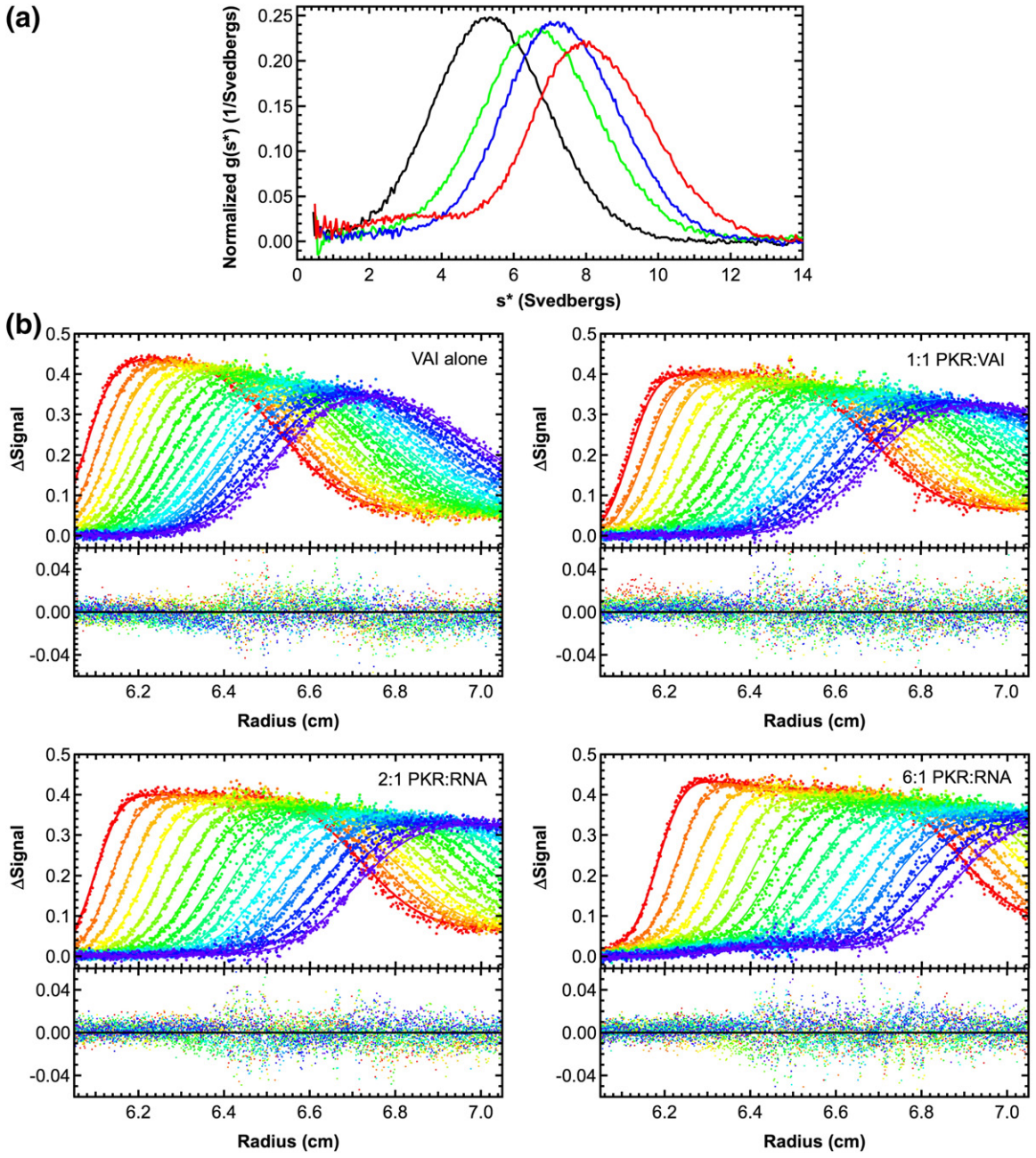

Fig. 2. Sedimentation velocity analysis of PKR binding to VAI. (a) Normalized $g(s^*)$ distributions of 0.4 μM VAI (black), VAI+1 Eq PKR (green), VAI+2 Eq PKR (blue), and VAI+6 Eq PKR (red). Distributions were calculated using DCDT+.[32] (b) Global analysis of difference curves. The data were subtracted in pairs to remove systematic noise, and the four data sets at the indicated PKR/VAI ratios were fitted to a 2:1 binding model using SEDANAL.[33] The fitted parameters were as follows: sedimentation coefficients of the complexes, VAI loading concentrations, and dissociation constants. The top panels show the data (points) and the fit (continuous lines), and the bottom panels show the residuals (points). The best-fit parameters are shown in Table 1. For clarity, only every-second difference curve is shown. Samples were prepared in a buffer consisting of 20 mM Hepes (pH 7.5), 200 mM NaCl, 0.1 mM ethylenediaminetetraacetic acid, and 0.01 mM Tris(2-carboxyethyl)phosphine (AU 200), and loaded into two-channel aluminum–epon double-sector cells equipped with quartz windows. Data were collected using absorbance optics in a Beckman Coulter XL-I analytical ultracentrifuge. Conditions: rotor speed, 35,000 rpm; temperature, 20 °C; wavelength, 260 nm.

Table 1. PKR–RNA interaction parameters derived from sedimentation velocity analysis

RNA	[Mg^{2+}] (mM)	Model	K_{d1} (nM)	K_{d2} (nM)	s(RNA)[a]	s(RP)[a]	s(RP_2)[a]	RMS[b]
VAI	0	R+P↔RP; RP+P↔RP_2	14 (3, 41)	601 (359, 1200)	5.34	6.78 (6.63, 7.04)	8.54 (8.30, 9.00)	0.00841
ΔTS	0	R+P↔RP	158 (136, 182)	—	4.33	6.43 (6.38, 6.48)	—	0.00854
VAI	5	R+P↔RP	334 (278, 401)	—	5.29	7.18 (7.07, 7.29)	—	0.00691
ΔTS	5	R+P↔RP	367 (302, 440)	—	4.38	6.19 (6.10, 6.29)	—	0.0104

Measurements were performed in AU 200 buffer or AU 200 buffer+Mg^{2+} at 20 °C at a rotor speed of 35,000 rpm (VAI and ΔTS). Parameters were obtained by global nonlinear least squares analysis of four samples at PKR/RNA ratios of 0, 1, 2, and 6 using SEDANAL.[34] The values in parentheses correspond to the 95% joint confidence intervals obtained using the *F*-statistic to define a statistically significant increase in variance[35] upon adjusting each parameter from its best-fit value.

[a] Uncorrected sedimentation coefficient (in Svedbergs).

[b] RMSD of the fit in absorbance units.

PKR binding and inhibitory potency are unaffected by the deletion of the entire terminal stem.[18] Isothermal titration calorimetry (ITC)[18,30,31] and gel-filtration measurements[18] indicate that VAI can bind multiple PKR monomers. However, the mechanism of inhibition by VAI remains unclear. It was reported that the isolated apical stem functions as a PKR activator, and that interactions with other regions of VAI mediate inhibition.[31] Alternatively, it was proposed that VAI functions by blocking PKR dimerization.[30] Here, we characterize PKR binding to VAI by sedimentation velocity measurements performed under the same conditions employed for enzymatic activity assays.

We have used sedimentation velocity analytical ultracentrifugation to define the stoichiometries and affinities of PKR binding to VAI and ΔTS, a VAI mutant that lacks the terminal stem (Fig. 1). The data were initially analyzed by the time derivative method to verify binding and to define the association model. Figure 2a shows that VAI has a sedimentation coefficient near 5 S, and the peak shifts to the right upon binding PKR. At the highest PKR concentration (6 Eq), the main peak is located near 8.5 S, with a shoulder near 3.5 S, corresponding to free PKR. Assuming a model of a single PKR molecule binding to VAI leads to a frictional ratio (f/f_0) estimate of 1.28, which is much lower than that of the RNA alone or those of other PKR–RNA complexes (Supplementary Material, Table S1). Therefore, we considered a model of two PKR molecules binding sequentially to VAI. The data fit well to this model in a global analysis of sedimentation velocity difference curves using SEDANAL (Fig. 2).[33] More reasonable f/f_0 values for the VAI–PKR complexes are obtained from this fit. As expected, a poor fit is obtained for a model of a single PKR monomer binding, with an RMS of 0.00946 and systematic deviations in the residuals. However, using a model of two PKR molecules binding results in an RMS of 0.00841 without significant systematic deviations (Fig. 2). The first PKR binds with high affinity (K_d=14 nM), and the second PKR binds with a lower affinity (K_d=600 nM) (Table 1). In contrast to wild-type VAI, only one PKR binds to the ΔTS mutant lacking the terminal stem. A dissociation constant of 158 nM (Table 1) lies between K_{d1} and K_{d2} for VAI. The fit quality is not improved by using a model that incorporates the binding of a second PKR, and the fitted sedimentation coefficients for the PKR–ΔTS complexes are unreasonable.

Because Mg^{2+} has been reported to affect VAI conformation,[23] we have analyzed the effects of divalent ion on the hydrodynamic properties of VAI and the binding of PKR. The uncorrected sedimentation coefficient of VAI decreases very slightly in the presence of Mg^{2+} (Table 1). However, this effect is due to the change in buffer density and viscosity; in both cases, f/f_0=1.61 (Supplementary Material, Table S1). Thus, Mg^{2+} does not induce a large-scale change in VAI conformation, which would affect the hydrodynamic properties of the RNA. The sedimentation velocity results are supported by small-angle X-ray scattering studies, where the radius of gyration (R_g) of VAI increases very slightly from 45.48±0.15 Å to 47.72±0.14 Å upon the addition of 5 mM Mg^{2+} (C.J.W., K.L.-F., and J.L.C., unpublished observations). Although Mg^{2+} does not induce significant structural changes, the affinity of PKR for VAI is strongly reduced by about 20-fold in the presence of 5 mM Mg^{2+}, and the second PKR binding event is not even detected (Table 1)†.

We have confirmed the sedimentation velocity results using ITC. In the absence of Mg^{2+}, a distinctly bimodal isotherm is observed, indicating that two PKR monomers bind to VAI under these conditions (Fig. 3). The dissociation constants obtained by fitting these data are in good agreement with those derived from sedimentation velocity. The enthalpy change for binding of the first PKR

† The Mg^{2+} concentration of 5 mM was chosen to match the conditions for PKR activity assays and is somewhat higher that the typical intracellular concentration (~0.5 mM Mg^{2+}).[36] We also detected a strong inhibition of the second PKR binding event by 0.5 mM Mg^{2+} (data not shown).

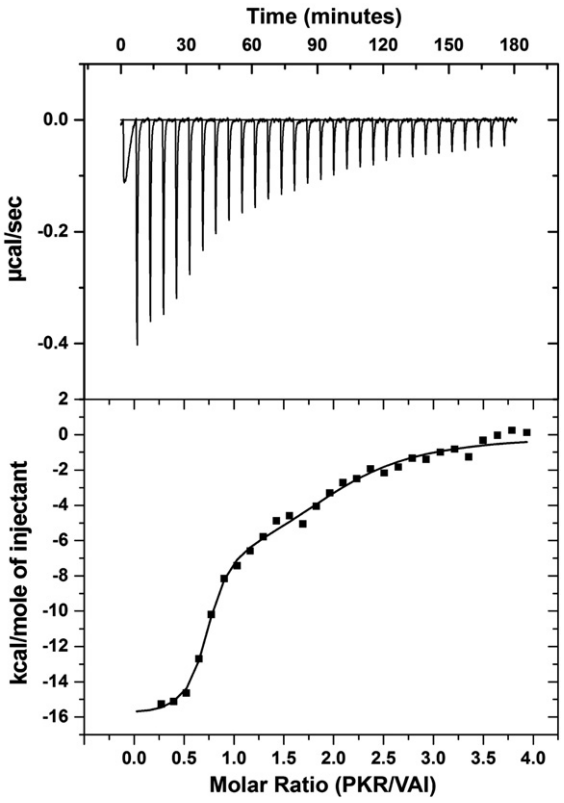

Fig. 3. ITC analysis of PKR binding to VAI. Measurements were performed using a VP-ITC calorimeter (Microcal, Inc.) at 20 °C. Both RNA and protein were exchanged in AU 200 buffer by exhaustive dialysis. The calorimeter cell contained 4 μM VAI, and the syringe contained 75 μM PKR. A single 2-μl injection was performed, followed by twenty-nine 10-μl injections. The top panel shows background-corrected ITC data, and the bottom panel shows integrated data (points) and the fit of the data to a model of two independent binding sites (continuous line) performed using ORIGIN (Microcal, Inc.) The best-fit parameters are shown in Table 2.

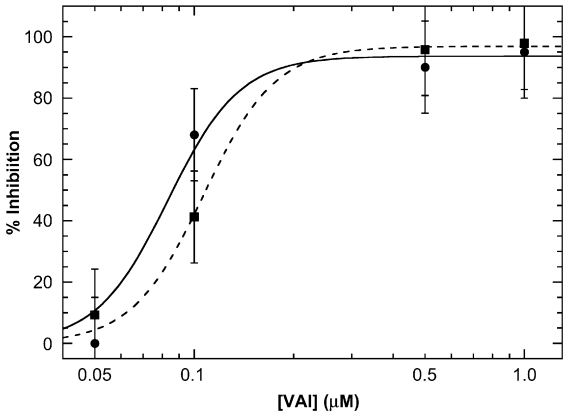

Fig. 4. Inhibition of the dsRNA activation of PKR by VAI (Circle) and ΔTS (Square). PKR autophosphorylation assays were performed, as previously described,[10,15] in AU 200 + 5 mM $MgCl_2$. PKR (100 nM) and variable concentrations of VAI were preincubated for 10 min at 30 °C, followed by addition of 10 μg/ml poly(rI:rC). After 20 min, 0.4 mM ATP containing 4 μCi of γ-^{32}P[ATP] was added, and the reaction was incubated for another 40 min before quenching with sample loading buffer. PKR autophosphorylation was quantified by PhosphorImager analysis and referenced to samples containing no inhibitor. Each point represents the average of three measurements, and error bars indicate the estimated standard error.

is about twice that of the second PKR. In the presence of Mg^{2+}, only one PKR binds (Fig. S1); again, the K_d values agree well with the previous results in Table 2. The large enthalpy change correlates with the first high-affinity PKR binding event observed in the absence of Mg^{2+}.

To validate the functional relevance of the sedimentation velocity and ITC experiments performed in the presence of Mg^{2+}, we performed enzymatic activity assays under the same conditions used for biophysical measurements. Figure 4 shows the inhibition of dsRNA-induced PKR autophosphorylation by wild-type VAI and ΔTS. Both RNAs effectively inhibit this reaction; within error, their apparent potencies are about the same. Consistent with the present data, it has previously been reported that the central domain and the apical stem comprise the PKR binding regions of VAI,[17,20,21,23,25–29] and deletion of the terminal stem does not affect PKR-inhibitory potency.[18]

Although it is difficult to quantitatively analyze PKR activation kinetic data due to the existence of multiple phosphorylation sites and the complexity of autocatalytic reactions,[10] the fact that VAI and ΔTS completely inhibit autophosphorylation at concentrations above 0.5 μM is consistent with the PKR binding affinities determined for these RNAs in the presence of Mg^{2+} (Table 1). Note that divalent

Table 2. PKR–VAI interaction parameters derived from ITC analysis

[Mg^{2+}] (mM)	Model	K_{d1} (nM)	N_1	ΔH_1 (kcal/mol)	K_{d2} (nM)	N_2	ΔH_2 (kcal/mol)
0	R + P ↔ RP; RP + P ↔ RP_2	10±7	0.68±0.02	−15.9±0.5	794±367	1.34±0.10	−7.6±1.1
5	R + P ↔ RP	667±125	1.12±0.04	−13.2±0.5	—	—	—

ITC measurements were performed in AU 200 buffer or AU 200 buffer + Mg^{2+} at 20 °C. The parameters were obtained by global nonlinear least squares analysis of titration data using ORIGIN (Microcal, Inc.). The error ranges correspond to the values obtained with ORIGIN using the variance–covariance matrix and do not account for parameter correlation.

ion is required for PKR activity, so it is not possible to assess inhibition in the absence of Mg^{2+}. The inhibitory potency of VAI reported here is also consistent with previous studies where PKR inhibition is only detected at VAI concentrations above 100–300 nM.[18,26,30,34] Neither VAI nor ΔTS is capable of activating PKR in the absence of the dsRNA poly(rI:rC) (data not shown).

It is notable that Mg^{2+} strongly modulates the affinity of PKR for VAI. Typically, PKR binding is not dependent on divalent ion,[35] and the ~20-fold increase in K_d upon addition of Mg^{2+} is larger than expected from the slight increase in ionic strength. For example, the K_d for PKR binding to an unrelated 20-bp dsRNA increases only about 3-fold upon the addition of 5 mM Mg^{2+} in the presence of 200 mM NaCl (Supplementary Material, Table S2). Similarly, divalent ion only slightly reduces PKR binding affinity for ΔTS (Table 1). Thus, our data suggest that Mg^{2+} induces a change in the mechanism of PKR binding to VAI. This change is not reflected in the hydrodynamic properties of VAI (Table 1; Table S1), ruling out a large-scale rearrangement in VAI conformation. In thermal denaturation experiments, addition of Mg^{2+} induces an overall stabilization of VAI, but there is no evidence for specific interactions.[18,24] However, Mg^{2+} does alter the pattern of enzymatic cleavage and chemical modification within the VAI central domain.[23] Divalent ion is often required for the stabilization of the RNA tertiary structure, and we propose that Mg^{2+} is required for the correct folding of the VAI central domain. However, the nature of the structural change in VAI induced by Mg^{2+} is not clear, and further experiments are underway to probe the structure of the central domain and to define the role of divalent ion.

It is well established that dimerization plays a key role in the activation of PKR by RNA. Binding of multiple PKR monomers is required for the activation of PKR by both homogeneous duplex RNAs[15] and natural RNA hairpins that contain secondary structure defects.[14] Thus, we propose that VAI acts as an *in vivo* inhibitor of PKR because it binds only a single PKR under physiological conditions where magnesium is present. It was previously suggested that viral RNA inhibitors are capable of binding only one PKR monomer.[8] The high affinity of PKR for VAI or ΔTS is noteworthy. Typically, PKR binds most strongly to regions of homogeneous duplex RNAs, and secondary structure defects impede interaction. The apical stem consists of a stem loop with about 21 bp of duplex interrupted by two one-base bulges and three noncanonical base pairs, and the central domain contains a short stem loop with only 7 bp. PKR binds weakly to the isolated apical stem, with $K_d > 3$ μM in the presence of Mg^{2+} (K.L.-F. and J.L.C., unpublished observations). Thus, the highly structured central domain is likely responsible for mediating the high affinity of PKR for VAI and thus comprises a novel PKR binding motif.

Acknowledgements

This work was supported by National Institutes of Health grant AI-53615 to J.L.C. We thank Arlene Albert for providing access to the VP-ITC calorimeter.

Supplementary Data

Supplementary data to this article can be found online at doi:10.1016/j.jmb.2010.08.015.

References

1. Bowie, A. G. & Unterholzner, L. (2008). Viral evasion and subversion of pattern-recognition receptor signalling. *Nat. Rev. Immunol.* **8**, 911–922.
2. Toth, A. M., Zhang, P., Das, S., George, C. X. & Samuel, C. E. (2006). Interferon action and the double-stranded RNA-dependent enzymes ADAR1 adenosine deaminase and PKR protein kinase. *Prog. Nucleic Acid Res. Mol. Biol.* **81**, 369–434.
3. Weber, F., Wagner, V., Rasmussen, S. B., Hartmann, R. & Paludan, S. R. (2006). Double-stranded RNA is produced by positive-strand RNA viruses and DNA viruses but not in detectable amounts by negative-strand RNA viruses. *J. Virol.* **80**, 5059–5064.
4. Tian, B., Bevilacqua, P. C., Diegelman-Parente, A. & Mathews, M. B. (2004). The double-stranded RNA binding motif: interference and much more. *Nat. Rev. Mol. Cell Biol.* **5**, 1013–1023.
5. Nanduri, S., Carpick, B. W., Yang, Y., Williams, B. R. & Qin, J. (1998). Structure of the double-stranded RNA binding domain of the protein kinase PKR reveals the molecular basis of its dsRNA-mediated activation. *EMBO J.* **17**, 5458–5465.
6. Dar, A. C., Dever, T. E. & Sicheri, F. (2005). Higher-order substrate recognition of eIF2alpha by the RNA-dependent protein kinase PKR. *Cell*, **122**, 887–900.
7. VanOudenhove, J., Anderson, E., Krueger, S. & Cole, J. L. (2009). Analysis of PKR structure by small-angle scattering. *J. Mol. Biol.* **387**, 910–920.
8. Robertson, H. D. & Mathews, M. B. (1996). The regulation of the protein kinase PKR by RNA. *Biochimie*, **78**, 909–914.
9. Cole, J. L. (2007). Activation of PKR: an open and shut case? *Trends Biochem. Sci.* **32**, 57–62.
10. Lemaire, P. A., Lary, J. & Cole, J. L. (2005). Mechanism of PKR activation: dimerization and kinase activation in the absence of double-stranded RNA. *J. Mol. Biol.* **345**, 81–90.
11. Hunter, T., Hunt, T., Jackson, R. J. & Robertson, H. D. (1975). The characteristics of inhibition of protein synthesis by double-stranded ribonucleic acid in reticulocyte lysates. *J. Biol. Chem.* **250**, 409–417.

12. Manche, L., Green, S. R., Schmedt, C. & Mathews, M. B. (1992). Interactions between double-stranded RNA regulators and the protein kinase DAI. *Mol. Cell. Biol.* **12**, 5238–5248.
13. Kostura, M. & Mathews, M. B. (1989). Purification and activation of the double-stranded RNA-dependent eIF-2 kinase DAI. *Mol. Cell. Biol.* **9**, 1576–1586.
14. Heinicke, L. A., Wong, C. J., Lary, J., Nallagatla, S. R., Diegelman-Parente, A., Zheng, X. *et al.* (2009). RNA dimerization promotes PKR dimerization and activation. *J. Mol. Biol.* **390**, 319–338.
15. Lemaire, P. A., Anderson, E., Lary, J. & Cole, J. L. (2008). Mechanism of PKR activation by dsRNA. *J. Mol. Biol.* **381**, 351–360.
16. Langland, J. O., Cameron, J. M., Heck, M. C., Jancovich, J. K. & Jacobs, B. L. (2006). Inhibition of PKR by RNA and DNA viruses. *Virus Res.* **119**, 100–110.
17. Clarke, P. A., Pe'ery, T., Ma, Y. & Mathews, M. B. (1994). Structural features of adenovirus 2 virus-associated RNA required for binding to the protein kinase DAI. *Nucleic Acids Res.* **22**, 4364–4374.
18. Wahid, A. M., Coventry, V. K. & Conn, G. L. (2008). Systematic deletion of the adenovirus-associated RNAI terminal stem reveals a surprisingly active RNA inhibitor of double-stranded RNA-activated protein kinase. *J. Biol. Chem.* **283**, 17485–17493.
19. Coventry, V. K. & Conn, G. L. (2008). Analysis of adenovirus VA RNAI structure and stability using compensatory base pair modifications. *Nucleic Acids Res.* **36**, 1645–1653.
20. Furtado, M. R., Subramanian, S., Bhat, R. A., Fowlkes, D. M., Safer, B. & Thimmappaya, B. (1989). Functional dissection of adenovirus VAI RNA. *J. Virol.* **63**, 3423–3434.
21. Mellits, K. H. & Mathews, M. B. (1988). Effects of mutations in stem and loop regions on the structure and function of adenovirus VA RNAI. *EMBO J.* **7**, 2849–2859.
22. Ma, Y. & Mathews, M. B. (1996). Secondary and tertiary structure in the central domain of adenovirus type 2 VA RNA I. *RNA*, **2**, 937–951.
23. Clarke, P. A. & Mathews, M. B. (1995). Interactions between the double-stranded RNA binding motif and RNA: definition of the binding site for the interferon-induced protein kinase DAI (PKR) on adenovirus VA RNA. *RNA*, **1**, 7–20.
24. Coventry, V. K. & Conn, G. L. (2008). Analysis of adenovirus VA RNAI structure and stability using compensatory base pair modifications. *Nucleic Acids Res.* **36**, 1645–1653.
25. Mellits, K. H., Kostura, M. & Mathews, M. B. (1990). Interaction of adenovirus VA RNAI with the protein kinase DAI: nonequivalence of binding and function. *Cell*, **61**, 843–852.
26. Mellits, K. H., Pe'ery, T. & Mathews, M. B. (1992). Role of the apical stem in maintaining the structure and function of adenovirus virus-associated RNA. *J. Virol.* **66**, 2369–2377.
27. Ghadge, G. D., Malhotra, P., Furtado, M. R., Dhar, R. & Thimmapaya, B. (1994). *In vitro* analysis of virus-associated RNA I (VAI RNA): inhibition of the double-stranded RNA-activated protein kinase PKR by VAI RNA mutants correlates with the *in vivo* phenotype and the structural integrity of the central domain. *J. Virol.* **68**, 4137–4151.
28. Rahman, A., Malhotra, P., Dhar, R., Kewalramani, T. & Thimmapaya, B. (1995). Effect of single-base substitutions in the central domain of virus-associated RNA I on its function. *J. Virol.* **69**, 4299–4307.
29. Spanggord, R. J. & Beal, P. A. (2001). Selective binding by the RNA binding domain of PKR revealed by affinity cleavage. *Biochemistry*, **40**, 4272–4280.
30. McKenna, S. A., Lindhout, D. A., Shimoike, T., Aitken, C. E. & Puglisi, J. D. (2007). Viral dsRNA inhibitors prevent self-association and autophosphorylation of PKR. *J. Mol. Biol.* **372**, 103–113.
31. McKenna, S. A., Kim, I., Liu, C. W. & Puglisi, J. D. (2006). Uncoupling of RNA binding and PKR kinase activation by viral inhibitor RNAs. *J. Mol. Biol.* **358**, 1270–1285.
32. Philo, J. S. (2006). Improved methods for fitting sedimentation coefficient distributions derived by time-derivative techniques. *Anal. Biochem.* **354**, 238–246.
33. Stafford, W. F. & Sherwood, P. J. (2004). Analysis of heterologous interacting systems by sedimentation velocity: curve fitting algorithms for estimation of sedimentation coefficients, equilibrium and kinetic constants. *Biophys. Chem.* **108**, 231–243.
34. Pe'ery, T., Mellits, K. H. & Mathews, M. B. (1993). Mutational analysis of the central domain of adenovirus virus-associated RNA mandates a revision of the proposed secondary structure. *J. Virol.* **67**, 3534–3543.
35. Bevilacqua, P. C. & Cech, T. R. (1996). Minor-groove recognition of double-stranded RNA by the double-stranded RNA-binding domain of the RNA-activated protein kinase PKR. *Biochemistry*, **35**, 9983–9994.
36. Gunther, T. (2006). Concentration, compartmentation and metabolic function of intracellular free Mg^{2+}. *Magnesium Res.* **19**, 225–236.